

Highlights

Reducing RES Droughts through the integration of wind and solar PV

Boris Morin, Aina Maimó Far, Damian Flynn, Conor Sweeney

- RES droughts are analysed using 45 years of hourly wind and solar PV generation data
- RES droughts from C3S-Energy and ERA5-Atlite datasets are compared
- Adding solar PV to a wind-dominated system reduces RES drought frequency and duration
- Validated RES datasets are crucial to accurately identify RES drought extremes

Reducing RES Droughts through the integration of wind and solar PV

Boris Morin^{a,*}, Aina Maimó Far^a, Damian Flynn^b, Conor Sweeney^a

*^aSchool of Mathematics and Statistics, University College Dublin, Belfield, Dublin
4, Dublin, D04 V1W8, Ireland*

*^bSchool of Electrical and Electronic Engineering, University College Dublin, Belfield,
Dublin 4, Dublin, D04 V1W8, Ireland*

*Corresponding author

Email addresses: `boris.morin@ucdconnect.ie` (Boris Morin),
`aina.maimofar@ucd.ie` (Aina Maimó Far), `damian.flynn@ucd.ie` (Damian Flynn),
`conor.sweeney@ucd.ie` (Conor Sweeney)

Abstract

Increasing the share of electricity produced from renewable energy sources (RES), combined with RES dependence on weather, poses a critical challenge for energy systems. This study investigates the importance of the balance between wind and solar photovoltaic (PV) capacity on periods of low renewable generation, known as RES droughts. Three different RES datasets are used to estimate the capacity factors for different scenarios of installed capacities for wind and solar PV power. The skill of the RES datasets is quantified by comparing capacity factor time series to observed hourly data and by assessing their representation of observed RES droughts. The RES datasets are used to generate a 45-year hourly time series of RES capacity factor, enabling analysis of the frequency, duration and return periods of RES droughts at a climatological scale. Results show the importance of using an accurate, validated RES dataset for RES drought risk assessment. The addition of solar PV capacity to a wind-dominated system results in a significant reduction in the frequency and duration of RES droughts, while also reducing extremes and seasonal RES drought patterns. These findings underscore the importance of diversification in RES capacity to enhance energy security and resilience.

Keywords: RES Drought, Wind Power, Solar PV Power, Renewable Energy Sources, Return Periods

1. Introduction

The EU aims to generate at least 69% of its electricity from renewable energy sources (RES) by 2030, up from 41% in 2022 [1]. While this transition is essential for reducing greenhouse gas emissions, it also highlights the challenge of managing the variability of weather-dependent energy sources such as wind and solar photovoltaic (PV) power. This challenge is amplified by the increasing electrification of energy sectors, which places greater demand on the power system and makes it more sensitive to meteorological conditions [2]. Periods of low renewable generation, known as *Dunkelflaute* or RES droughts, pose significant risks to system adequacy and energy security, emphasising the need for a resilient energy system to meet both growing electricity demand and decarbonisation targets.

RES drought events do not have a fixed definition, with various approaches present in the literature. One common method defines a RES drought as a period during which the average capacity factor (CF) remains below a fixed threshold for a specified duration. For example, Kaspar et al. [3] used this method to investigate the shortfall risks of low wind and solar PV generation in Europe, with a focus on Germany, testing multiple CF thresholds and durations. Similarly, Mockert et al. [4] examined the link between weather regimes and RES droughts in Germany using a 48-hour rolling window under a threshold to define RES droughts. Similar fixed-threshold approaches have also been applied using CF series reconstructed through machine learning in regions such as Japan [5] and Hungary [6].

Alternative methods adjust the CF threshold dynamically over the year to account for seasonal variations in renewable production. Raynaud et al. [7] defined RES droughts as sequences of days with renewable electricity generation below a threshold that varies seasonally, a methodology later adapted for India [8]. Building on this, Kapica et al. [9] compared the likelihood of increased RES droughts in Europe under different climate models. Other studies have defined RES droughts based on deviations from daily mean production: Rinaldi et al. [10] applied these in the U.S. Western Interconnection to quantify the benefits of long-term storage, while Brown et al. [11] examined weekly timescales to explore meteorological influences on the most severe RES drought events. Another method defines RES drought indices based on metrics commonly used in hydro-meteorology to characterise RES droughts [12]. This approach identifies periods of unusually low generation relative to historical production levels, using the lowest production percentiles. Bracken et al. [13] used this approach to analyse RES droughts at different time scales in the U.S. [13], and Lei et al. [14] used it to quantify RES droughts in wind-PV-hydro systems in China.

In addition to examining periods of low renewable electricity generation, several studies also explore the periods when the imbalance between renewable generation and electricity demand (residual demand) is high. Raynaud et al. [7] showed the difference between RES droughts and high residual demand events in a hypothetical fully renewable system composed of wind, solar PV and run-of-the-river hydropower. Similarly, Allen and Otero [12] also defined a standardised index based on meteorological droughts to address residual demand, whose correlation to the electricity generation index is mostly negative (as expected, although quite low anticorrelations and even small positive correlations appear for some European countries). This index

51 was also applied to the U.S. by Bracken et al. [13], revealing a consistent
52 increase in the RES drought magnitude when demand is considered, despite
53 showing differing results across regions.

54 In this paper, the focus is exclusively on renewable electricity generation,
55 to keep the focus on RES droughts driven by the weather. A fixed threshold
56 approach is used to define RES droughts, which facilitates consistent inter-
57 comparison between scenarios with different installed wind and solar PV
58 capacities. The case study used in this paper is Ireland, a region where
59 most RES generation comes from wind power and with ambitious targets for
60 solar PV power expansion. This provides valuable insights into the potential
61 benefits of adding solar PV installations in wind-dominated countries.

62 RES droughts are identified using onshore wind and solar PV CF time
63 series. In this study, three different datasets are used and compared, all of
64 which are driven by the ERA5 reanalysis [15]. Two of the datasets are part
65 of C3S Energy (C3SE), an energy-based operational dataset produced by
66 the EU Copernicus Climate Change Service [16]. One of the C3SE datasets
67 provides CF time series aggregated at the national scale, while the other
68 provides the CF time series at each grid point, at the ERA5 resolution of
69 0.25° . The third dataset produced by the authors was generated using the
70 Atlite model [17], which converts the ERA5 atmospheric data to a generation
71 time series using specified wind turbine and PV panel models. Atlite is an
72 open-source tool developed by PyPSA [17] and has been used for estimating
73 wind and solar PV generation in order to study RES droughts in Germany [4].

74 Generic datasets for wind and solar PV CF are often used for the quan-
75 tification of RES droughts. Despite undergoing a general validation process,
76 they are often not fully representative of each geographical location, and can
77 show differences in the number of RES drought events subsequently iden-
78 tified [18]. This study evaluates the skill of a dataset developed for the
79 European region (C3SE) when applied to a specific country; Ireland, repre-
80 sentative of Northwestern Europe. In particular, the analysis explores the
81 impact of using a generic versus a tailored dataset on RES drought assess-
82 ments, in the context of a transition from a wind-dominated system to one
83 with a greater share of solar PV capacity.

84 The aim of this study is to answer two questions which are relevant for
85 systems with a large share of RES generation:

- 86 • Do generic datasets have sufficient skill to reliably quantify RES drought
87 events for specific countries?

- How does the integration of solar PV capacity into a predominantly wind-based system alter the characteristics of RES drought events?

The datasets used in this study are detailed in section 2, which describes their characteristics and relevance for evaluating RES droughts. Section 3 outlines the RES datasets used to simulate wind and solar PV generation and provides the methodology for defining and identifying RES drought events, including the thresholds and metrics applied. In section 4, the datasets are first verified against observed energy data to assess their accuracy, followed by an analysis of RES drought occurrences for two scenarios with different ratios of installed wind to solar PV capacities. Finally, section 5 offers a discussion of the results in the context of energy reliability and future planning, followed by the main conclusions and recommendations for further research.

2. Data

This study uses publicly available datasets to construct and validate the datasets for estimating the CF of wind and solar PV power. The primary data sources include: EirGrid and SONI, the transmission system operators (TSO) for the Republic of Ireland and Northern Ireland, respectively; the ERA5 reanalysis dataset; and the C3SE dataset.

2.1. Wind and solar PV Capacity and Availability

EirGrid, the TSO for the Republic of Ireland, and SONI, the Northern Ireland TSO, provide detailed datasets on all wind and solar PV farms across the island of Ireland (Republic of Ireland and Northern Ireland) from 1990 to the present [19]. These datasets include information such as each farm’s installed capacity, name, and connection date. To enhance the accuracy of this data, the longitude and latitude for each farm were manually determined through online searches. For simplicity, this data will be referred to as originating from EirGrid, as all-island data was directly obtained from EirGrid, and the combined regions of the Republic of Ireland and Northern Ireland will be referred to as Ireland throughout the remainder of this document.

The spreadsheet available from the EirGrid website contains two key variables: generation and availability. Generation and availability values are available from 2014 onward for wind power and from 2018 onward for solar PV power, although solar PV availability data only became present in the Republic of Ireland in 2023. Generation is the energy that a RES farm actually contributed to the grid, which may include limitations introduced by the

123 TSO to maintain grid stability, such as constraints and curtailment. Avail-
 124 ability represents the energy that would have been generated from a RES
 125 farm if no grid constraints had been applied, making it representative of the
 126 weather-related response. This study focuses on availability for all analyses.

127 2.2. Atmospheric Variables

128 All of the datasets used in this study are driven by data from the ERA5 re-
 129 analysis [15], produced by the European Centre for Medium-Range Weather
 130 Forecasts (ECMWF). This global gridded dataset provides hourly atmo-
 131 spheric variables from 1940 to the present at a horizontal resolution of 0.25°.
 132 Table 1 lists the relevant ERA5 variables.

Table 1: ERA5 variables used to calculate wind and solar PV generation

ERA5 name	variable
100 metre zonal and meridional wind speed	u_{100}, v_{100}
2 metre temperature	$t2m$
Surface net solar radiation	ssr
Surface solar radiation downwards	$ssrd$
Top of atmosphere incident radiation	$tisr$
Total sky direct solar radiation at surface	$fdir$

133 2.3. C3S Energy

134 The EU Copernicus Climate Change Service developed the C3S-Energy
 135 (C3SE) renewable energy dataset for Europe [16], using ERA5 atmospheric
 136 variables and weather-to-energy models. This dataset provides hourly CF for
 137 wind and solar PV power from 1979 to the present. The data are available
 138 on the same grid as the ERA5 data, which has a horizontal resolution of
 139 0.25°. The time series are also available for download at two aggregated
 140 scales: regional (NUTS 2) and national.

141 The wind CF in C3SE was calculated using wind speeds at 100 m (u_{100} ,
 142 v_{100}) and a standard wind turbine model, the Vestas V136/3450, with a fixed
 143 hub height of 100 m. As data on wind turbine fleet locations and specifi-
 144 cations are difficult to obtain across Europe, C3SE assumes a homogeneous
 145 distribution of wind turbines across the ERA5 grid. While this approach
 146 does not capture the precise capacity factors reported by grid operators, it
 147 provides a well-correlated time series that effectively represents the impact

of weather variability on wind power generation. The C3SE solar PV CF was also calculated for the ERA5 grid. It is derived from meteorological data, including surface solar radiation downwards (*ssrd*) and air temperature (*t2m*), using a reference solar PV plant model. This model incorporates empirical calculations for key system components, such as optical losses, the electrical characteristics of the power module and the power curve of the PV inverter. The final CF accounts for a mix of module orientations typical for each location [20].

3. Methods

This study analyses RES droughts using onshore wind and solar PV CF time series from three datasets: two from C3SE; one based on national-level data (C3S NAT) and the other on grid-level data (C3S GRD), and a third dataset derived using the Atlite model (ATL).

3.1. C3S Energy National: C3S NAT

The C3S NAT dataset is created by combining two inputs provided by C3SE at the corresponding NUTS levels: Republic of Ireland (NUTS0: IE) and Northern Ireland (NUTS2: UKN0). The two inputs are combined, using the actual installed capacity as weights. This dataset assumes that RES generation occurs at every ERA5 grid point in Ireland.

3.2. C3S Energy Gridded: C3S GRD

The C3S GRD dataset uses, as inputs, the actual locations of the RES farms in Ireland, and the CF from C3SE over the ERA5 grid. For each farm, the CF from the nearest grid point on the C3SE dataset was selected. A weighted average of the CF associated with each farm, using the farm's installed capacities, was used to produce the combined CF time series.

3.3. Atlite: ATL

The ATL dataset is produced using the Atlite model. Atlite allows the user to define the wind turbine power curve and PV panel model to use when converting weather variables to wind and solar PV generation. The Atlite model takes as inputs the locations of RES farms and ERA5 weather variables: wind speed at 100 m (u_{100} , v_{100}) for wind generation, and radiation variables (*ssr*, *ssrd*, *tisr*, and *fdir*) along with air temperature (*t2m*) for solar PV generation. The output of the Atlite model is a generation time

series, which is divided by the total capacity to transform it back into a CF. The selection of the wind turbine power curve and PV panel model represents the key difference between this dataset and C3S GRD. This study identifies the most appropriate wind turbine power curve to use from the 121 power curves, each at five different levels of smoothing, made available by Renewables.ninja [21], and selects the PV panel model out of the options available within Atlite.

3.4. Energy Scenarios

The three datasets provide time series for both wind and solar PV CF. In addition to analysing the CF of wind and solar PV separately, a combined CF was computed for each dataset by averaging wind and solar PV CF, weighted by their installed capacities at the end of 2023 (5.9 GW for wind power and 0.6 GW for solar PV power). This configuration is referred to as the 91W-9PV scenario, reflecting the distribution of 91% wind and 9% solar PV capacity. Given that solar PV capacity in Ireland is low in 2023, and to explore how a more balanced distribution of wind and solar PV capacities might impact RES droughts, this study also considered a second scenario, referred to as 57W-43PV, where the installed solar PV capacity is assumed to increase to 8.6 GW, while wind capacity rises to 11.45 GW. These values are based on targets outlined in the roadmap published by the 2024 Climate Action Plan [22]. This study does not include offshore wind in the analysis. Recent reports suggest that even by 2030, Ireland is unlikely to have any significant new offshore wind farms, with projected offshore capacity expected to remain near zero using realistic scenarios [23].

New time series were generated for both the ATL and C3S GRD solar PV datasets, incorporating a revised distribution of installed capacity across Ireland as specified in the roadmap [24]. For wind power, the CF time series remains unchanged, as significant shifts in the location of wind farms are not expected. In total, twelve CF time series were analysed in this study, six for individual wind and solar PV CF (three datasets for each source) in the 91W-9PV scenario, and an additional six time series that include the combined CF for 91W-9PV and 57W-43PV scenarios across the different datasets.

It is important to note that the specific capacity values used in this study are illustrative and are not intended to reflect accurate future realities. Instead, they serve to explore the impact of transitioning from a wind-dominated system (91W-9PV) to a more evenly distributed system (57W-43PV). This approach allows for a comparative analysis between the two

218 scenarios, assessing how the balance of RES capacity affects the occurrence
219 of RES droughts.

220 In summary, for each of the three datasets (ATL, C3S GRD and C3S
221 NAT) four energy scenarios are examined:

- 222 • Wind Power - based on actual capacity at the end of 2023
- 223 • Solar PV Power - based on actual capacity at the end of 2023
- 224 • Combined RES / 91W-9PV - based on actual capacity at the end of
225 2023
- 226 • Combined RES / 57W-43PV - based on projected capacity for 2030

227 3.5. RES Drought Definition

228 In this study, a RES drought event was defined as occurring when the
229 24-hour moving average of CF remains below a fixed threshold of 0.1 for a
230 period of longer than 24 hours. By using a 24-hour moving average, fewer
231 but longer-lasting events were captured compared to using the raw CF time
232 series, which can be more sensitive to short-term fluctuations. The 24-hour
233 rolling average also avoids potential masking of day-long events due to their
234 start time. A fixed threshold approach was chosen in this study to enable
235 consistent inter-comparison between datasets.

236 The moving average approach smooths out short-term fluctuations, so
237 that brief periods above the threshold do not interrupt an otherwise continu-
238 ous low-CF period (Fig. 1). This means that a single hour above the threshold
239 does not "break" a RES drought event if it is surrounded by prolonged low-
240 generation hours. As a result, fewer but longer-lasting RES drought events
241 are identified, which may better reflect actual conditions where energy supply
242 constraints persist over extended periods.

243 4. Results

244 4.1. Verification

245 The accuracy of the datasets used in this study was verified against na-
246 tional generation data, before continuing to the analysis of RES droughts.
247 For the verification process, time varying values of installed capacity were
248 used to account for changes in RES development over the verification pe-
249 riod. This validation step evaluates how well the datasets represent actual

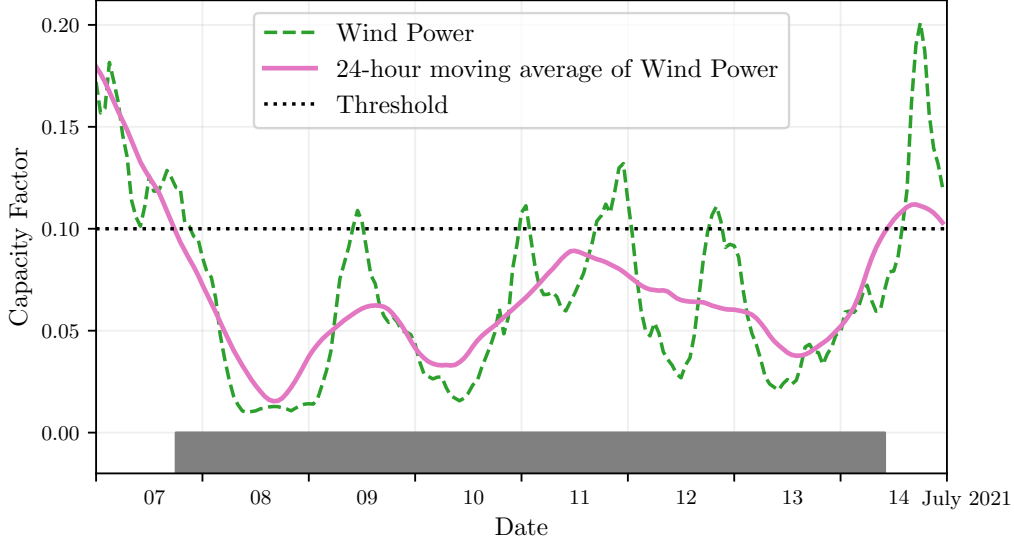


Figure 1: Wind time series of CF (green) and its 24-hour moving average (pink) from the 7th to the 15th of July 2021. The black dashed line indicates the CF threshold. The grey bar shows the period identified as a wind drought under our definition

renewable generation profiles by comparing them against observed data. The overall statistical distribution of CF values for wind (2014–2023) and solar PV (2023) is presented in the violin plots in Fig. 2. These plots illustrate the density of CF values for each dataset, highlighting their differences and alignment with observations. The results indicate that ATL aligns more closely with observations for wind, while all datasets exhibit similar distributions for solar PV.

4.1.1. Wind Energy

The C3S datasets use the Vestas V136/3450 wind turbine power curve (Fig. 3a). The Atlite model allows the user to specify the power curve. We considered the 121 power curves available for download from Renewables.ninja [21]. For each power curve, Renewables.ninja also provides four associated smoothed power curves. The smoothing is done using a Gaussian filter with different standard deviations that depend on the wind speed. A separate wind CF time series for Ireland was generated for each of the wind turbine power curves and smoothing levels.

The performance of each CF time series is then assessed based on four skill

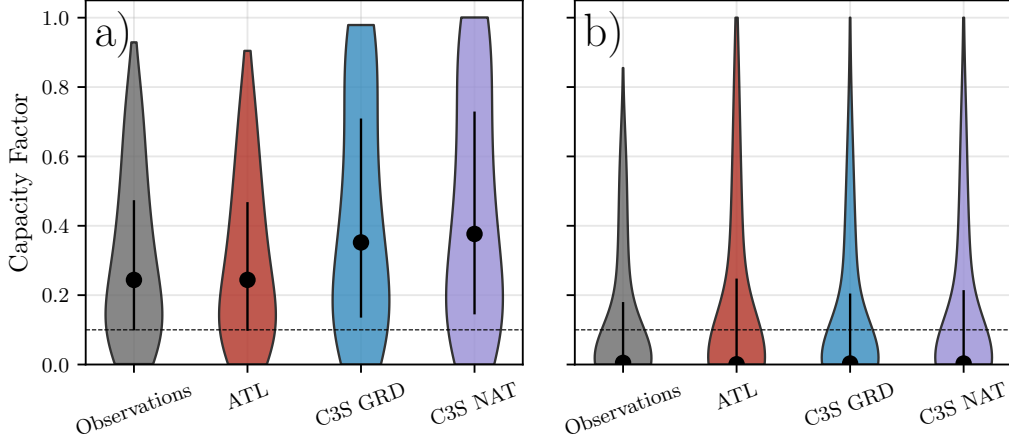


Figure 2: Violin plots of CF distributions for a) wind and b) solar PV for the Observations (grey) and the three datasets: ATL (red), C3S GRD (blue), and C3S NAT (purple). The black dot shows the median values, while the black vertical lines represent the first and third quartiles. The black dashed line indicates the threshold of 0.1 used in the study to identify RES droughts

267 scores: correlation coefficient (CC), root mean square error (RMSE), mean
 268 bias error (MBE), and the percentage of overlap. The percentage of overlap
 269 quantifies the similarity between the observed and modelled distributions. It
 270 is a positively oriented skill score, where 100% shows full agreement between
 271 the two distributions, and 0% indicates no overlap. The histograms of hourly
 272 CF values for the most recent decade (2014-2023) are used to calculate this
 273 skill score.

274 Based on these metrics, the most representative power curve for Ireland
 275 is the Enercon E112.4500 power curve with the $0.3w$ smoothing filter. The
 276 smoothing of the wind turbine power curve represents losses associated with
 277 each turbine, as well as losses such as wake effects between turbines, which
 278 are important when modelling wind energy on larger spatial scales. The
 279 histogram in Fig. 3b shows that the C3SE power curve tends to underestimate
 280 low CF values and overestimate higher ones, whereas the smoothed ATL
 281 power curve more closely follows the observed wind availability data. This
 282 is further supported by the percentage of overlap which is higher for ATL
 283 (97.2%) than for C3SE (83.2%), indicating better agreement with observed
 284 data.

285 The effect of the difference between the power curves is also visible in

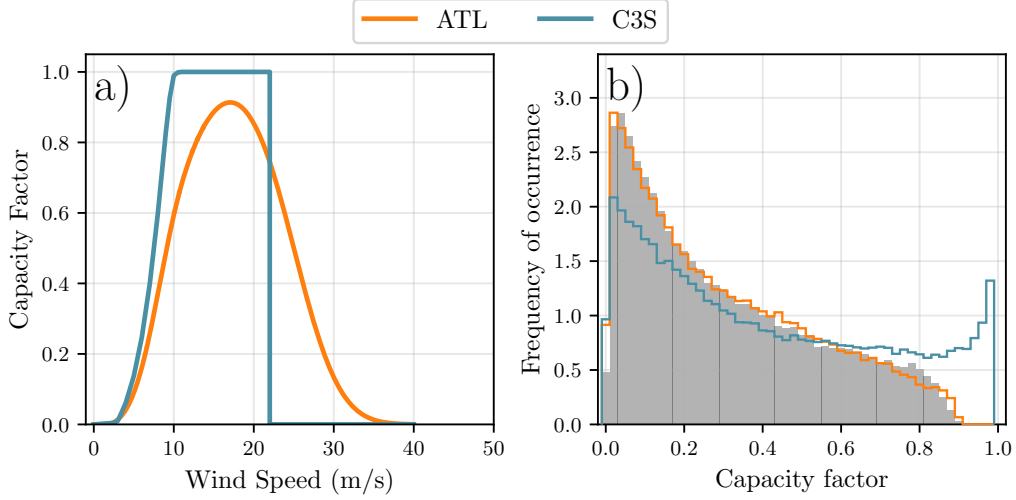


Figure 3: a) Power curves of the Enercon E112.4500 with a 0.3w smoothing filter used by the ATL dataset (orange) and the Vestas V136/3450 used by the two C3S datasets (blue) b) Histograms of wind CF for Ireland for the ATL dataset (orange), the C3S datasets (blue) and Observed (shaded)

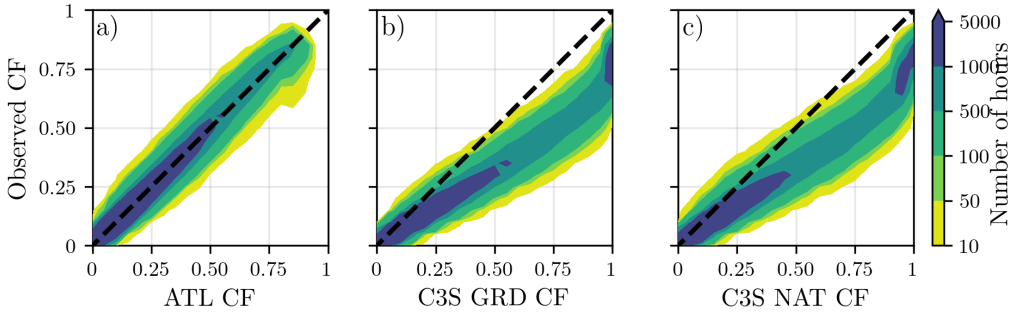


Figure 4: Wind CF density plot of the observed CF (vertical axes) and modelled (horizontal axes) CF data for the a) ATL, b) C3S GRD and c) C3S NAT datasets

286 Fig. 4, which shows a density plot of wind CF values. The two C3S datasets
 287 are shown to overestimate the observed CF, whereas the ATL dataset is in
 288 good agreement with the observed data. The skill scores presented in Table 2
 289 show that ATL performs better than the two C3S datasets for all of the skill
 290 scores.

291 Fig. 5 shows the average annual number of wind drought events during

	ATL	C3S GRD	C3S NAT
CC	0.981	0.972	0.970
RMSE	0.045	0.177	0.162
MBE	-0.003	0.137	0.121

Table 2: Skill scores for wind power for the three datasets compared to observed data

the 2014 to 2023 validation period. The figure reveals that ATL presents the best overall agreement with the observed frequency and duration of wind drought events. This pattern is particularly evident for shorter-duration events, which are the most frequent.

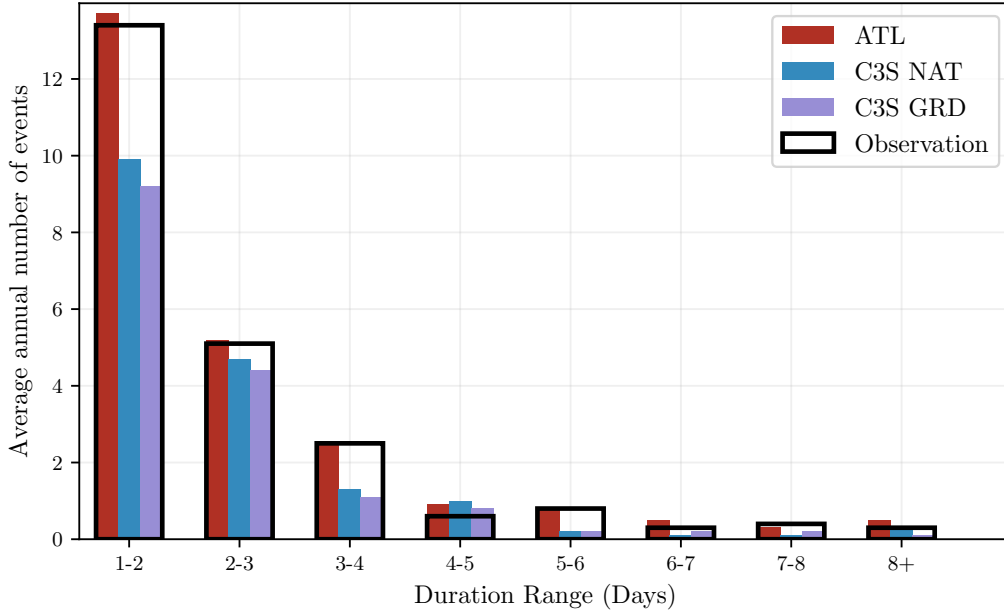


Figure 5: Average annual number of wind drought events for ATL (red), C3S GRD (blue), C3S NAT (purple), and the observed data (black outline). The wind droughts are identified from 2014 to 2023, considering the actual capacity of the system at any given time

Verification of wind generation data highlights the importance of selecting a representative wind turbine power curve for the region being analysed. The ATL dataset, which uses a representative wind turbine power curve, is skilled at reproducing wind CF and RES droughts across Ireland. On the other hand, the power curve used for both C3S GRD and C3S NAT is not

representative for Ireland, as it severely overestimates generation, underestimating the occurrence of RES droughts. This highlights a problem with using generalised datasets for analysing RES droughts: biases severely affect their ability to accurately reproduce RES drought events. The skill scores for the three datasets (Table 2) show only a small difference in their ability to reproduce the changes in CF, as seen by their similar CC scores. However, their ability to reproduce the actual CF values is much lower than that for ATL, with RMSE scores almost four times higher than for the two C3S datasets. There is a clear bias towards an overestimation of CF, seen in the MBE values, which leads to an underestimation of RES droughts, which highlights the strong motivation to use regionally verified models to assess RES droughts.

4.1.2. Solar PV Energy

The Atlite model allows the user to select certain PV panel characteristics. In this study, the three PV panel types available in the Atlite model were considered (CSi, CdTe, Kaneka). Following the same methodology as in the previous section, the three available models were compared using four skill scores (CC, RMSE, MBE, and the percentage of overlap). Based on the best-performing metrics, the Beyer PV panel model was selected [25], using the Kaneka Hybrid panel option. For all solar PV farm locations, the azimuth angle is fixed at 180° (due south), and the optimal tilt angle option is applied.

The solar PV installed capacity available on the spreadsheets from EirGrid represents the Maximum Export Capacity (MEC) and does not accurately reflect the installed solar PV capacity. To enable actual solar PV generation potential to be modelled correctly, installed capacities were set at 1.4 times the MEC values. This scaling factor was estimated by analysing proprietary data from individual solar PV farms provided by EirGrid, which showed that, on average, assuming that the installed capacities of farms exceed their MEC values by 40% yields the best agreement with the observed availability.

Fig. 6 shows that the three datasets have a similar tendency to overestimate the CF compared to the observed values, especially for high CF values. The skill scores presented in Table 3 indicate that C3S GRD and C3S NAT perform better than ATL for solar PV CF, with lower RMSE and MBE, and higher CC scores. This may be due to the statistical approach taken by C3SE for the orientation of the PV panels.

Fig. 7 shows the number of solar PV drought events during the 2023

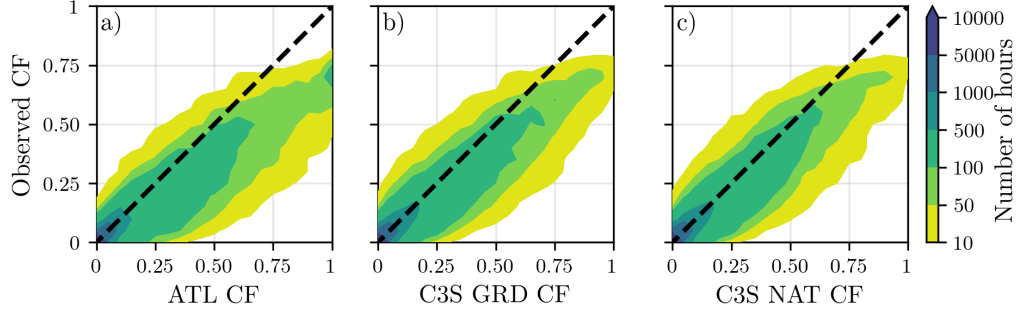


Figure 6: Solar PV CF density plot of the observed (vertical axes) and modelled (horizontal axes) CF series for the a) ATL, b) C3S GRD and c) C3S NAT datasets

	ATL	C3S GRD	C3S NAT
CC	0.921	0.931	0.931
RMSE	0.119	0.090	0.113
MBE	0.046	0.027	0.021

Table 3: Skill scores for solar PV CF for the three datasets compared to observed data

validation period across different duration ranges. The figure reveals partial agreement between the three datasets and the observed data, with consistent results noticed for duration ranges of 1-2, 3-4, 7-8, and 8+ days. However, discrepancies appear in the other ranges, where the datasets diverge from the observed data. The main challenge in validating solar PV data stems from the recent installation of a large share of Ireland's solar PV capacity, with over 65% of the total solar PV capacity installed in 2023. This results in uncertainties in solar PV generation data and the actual generating capacity in the first few months after each farm is connected. Overall, C3S GRD performs slightly better than the other datasets in reproducing observed solar PV drought events.

4.2. Analysis

In this section, RES droughts are analysed by calculating the frequency and duration of events, their return periods, and their seasonality. By examining both the frequency of occurrence and duration of these events, TSOs can better assess the need for alternative fossil fuel-based generation, long-duration energy storage, demand-side measures, and enhanced interconnections with neighbouring power systems to ensure adequate supply in a cost-



Figure 7: Number of solar PV drought events for ATL (red), C3S GRD (blue), and C3S NAT (purple) and the observed data (black outline). The solar PV droughts are identified for 2023, considering the actual capacity of the system at any given time

effective manner. Results are presented for the three datasets, which clearly illustrate how different modelling assumptions influence the characterisation of RES droughts.

RES drought events are evaluated under two different scenarios with fixed installed capacities: the 91W-9PV scenario, with 5.9 GW of wind capacity and 0.6 GW of solar PV capacity; and the 57W-43PV scenario, where wind capacity comprises 11.45 GW and solar PV capacity increases to 8.6 GW. Both scenarios were driven by 45 years of ERA5 data. Using the RES drought identification process described in Section 3.5, wind and solar PV droughts are first analysed separately before presenting the results for combined (wind + solar PV) RES droughts under both scenarios.

4.2.1. Annual Number of RES Droughts

The first part of the analysis examines the annual number of RES drought events. When only wind energy is considered (Fig. 8a), the number of RES drought events decreases as the duration range increases, with very few events lasting more than seven days. In contrast, for solar PV energy (Fig. 8b), RES

drought frequency declines from one to eight days and then slightly increases for longer durations. This behaviour is attributable to Ireland’s high-latitude location, where reduced sunlight in winter (from November to March) leads to consistently low solar PV output.

Moreover, the comparison between wind and solar PV results indicates that the median, first, and third quartiles for solar PV are consistently higher than or equal to those for wind. This is expected, given that solar PV generation is inherently lower, zero at night, and limited by the solar cycle. When wind and solar PV are combined under the 91W-9PV scenario (Fig. 8c), the results closely mirror those of wind alone, due to the dominance of wind power in the current energy mix. However, in the 57W-43PV scenario (Fig. 8d), a marked reduction in RES drought events is observed across all datasets, with a decrease of the total number of events of 56% for ATL, 52% for C3S GRD, and 50% for C3S NAT, demonstrating the beneficial effects of a more equal share of wind and solar PV capacity.

The consistently higher RES drought counts reported by the ATL dataset, compared to the C3S datasets, underscore the importance of wind turbine power curve representation when quantifying RES droughts. Whereas the three datasets agree on the overall effect of balancing the share of wind and solar PV generation, they differ at a quantitative level, which has crucial implications for energy planning.

4.2.2. Return Periods of RES Drought Duration

RES drought events identified over the 45-year period were used to calculate the return periods for different RES drought durations. A return period is the estimated average time interval between events of a specified duration (not to be confused with the frequency of their occurrence within a fixed time frame). Fig. 9 shows the return periods for different RES drought durations, which can be used to capture the most extreme events affecting the system. Understanding their return periods is crucial to inform decision makers about the trade-off between the risk of extreme events and the associated costs of mitigation measures. Extreme but rare RES droughts pose the toughest challenge to energy security by placing significant strain on the conventional backup sources necessary to maintain security of supply during these events.

The duration of wind droughts (Fig. 9a) increases in a log-linear fashion across the three datasets. The log-linear trend indicates a predictable relationship between wind drought duration and occurrence, with longer wind

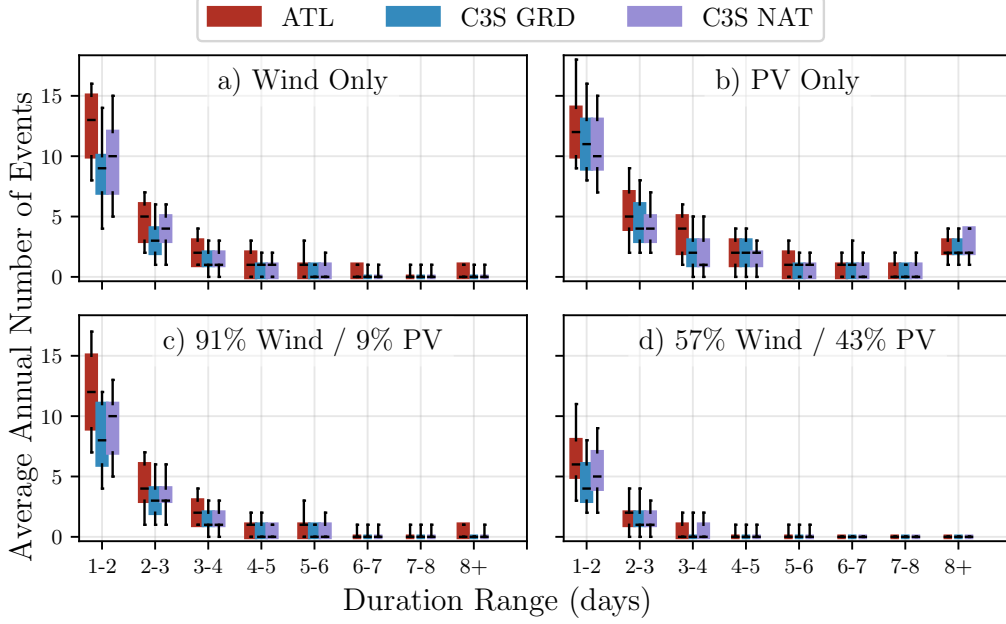


Figure 8: Average annual number of RES droughts (from 1979 to 2023) for a) Wind, b) solar PV, c) 91W-9PV and d) 57W-43PV for ATL (red), C3S GRD (blue), and C3S NAT (purple). The x-axis represents duration ranges in days (lower bound included), while the y-axis indicates the annual number of events. The boxes display the first and third quartiles and the median is marked by a black line. The whiskers indicate the 5th and 95th percentiles

409 droughts becoming exponentially less likely as duration increases. In the
410 case of solar PV droughts (Fig. 9b), Atlite behaves differently than the two
411 C3S datasets. The ATL dataset show a generally log-linear increase. For
412 C3S GRD and C3S NAT, the duration of PV droughts increases in a log-
413 linear pattern for events lasting less than 16 days. Beyond this duration,
414 there is a sharp rise in solar PV drought duration for events up to a one-year
415 return period. This sudden increase again reflects the impact of extended
416 periods of low PV generation during winter in Ireland. The difference be-
417 tween the ATL and the C3S results arises from differences in the datasets
418 near the threshold of 0.1 CF. ATL remains slightly above the threshold more
419 frequently during these conditions, leading to shorter, more fragmented RES
420 drought events. In contrast, C3S GRD and C3S NAT tend to fall below the
421 threshold in similar conditions, resulting in longer continuous RES drought

periods, especially during winter.

Under the 91W-9PV scenario (Fig. 9c), the combined RES drought return periods mirror those for wind alone, reflecting the dominance of wind in the current energy mix. In contrast, the 57W-43PV scenario (Fig. 9d) shows a dramatic reduction in RES drought durations, suggesting that a more balanced share of wind and solar PV capacity can substantially mitigate the frequency of prolonged RES drought events. For example, the return period for a five-day RES drought event (shown by the vertical dashed lines in Fig. 9) increases from roughly six months for the 91W-9PV scenario, to four years for the 57W-43PV scenario for the ATL dataset, and from about fifteen months to around five years for the two C3S datasets. This result indicates that the complementarity between wind and solar PV plays a crucial role in reducing the occurrence of RES drought events in a diversified energy portfolio.

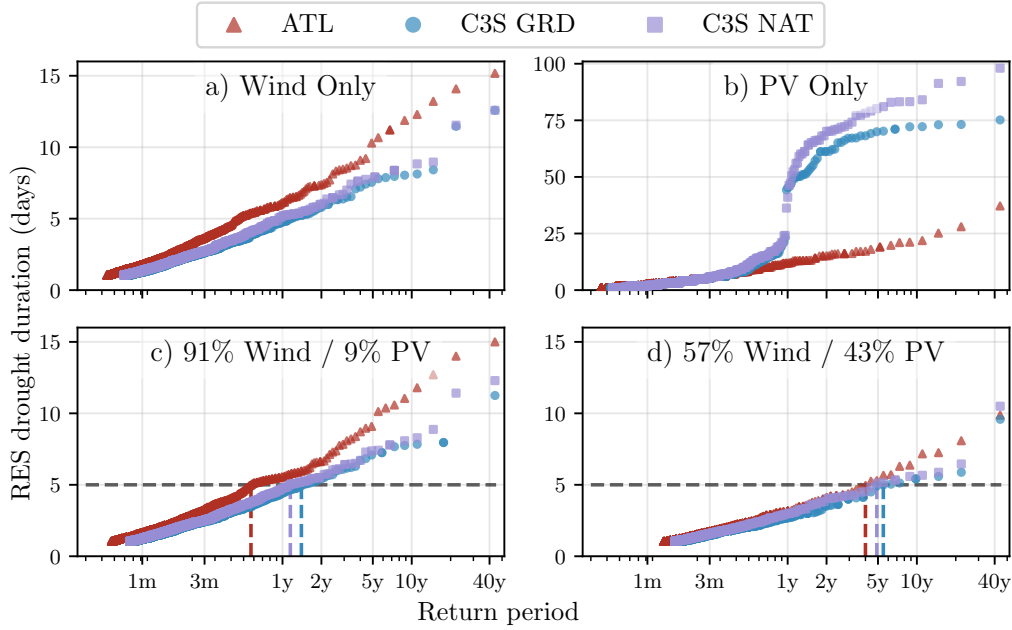


Figure 9: Return periods of the duration of RES droughts (from 1979 to 2023) for a) Wind, b) Solar PV, c) 91W-9PV and d) 57W-43PV for ATL (red triangle), C3S GRD (blue circle), and C3S NAT (purple square). The x-axis represents the return period time in a log-scale and the y-axis indicates the duration of RES drought associated with it. The horizontal dashed line marks the 5-day return period, with coloured vertical dashed marking its return period for each dataset

Across Fig. 9a, c, and d, the return periods in the ATL dataset are consistently higher than those in the two C3S datasets. For instance, in the 91W-9PV scenario (Fig. 9c), an event with a one-year return period lasts six days in the ATL dataset, compared to only five days in the C3S datasets. This difference underscores the importance of dataset selection when quantifying RES droughts, as each dataset’s assumptions and parametrisations significantly influence RES drought duration estimates. Additionally, in all four graphs, the similarity between results from the two C3S datasets suggests that assumptions in the ATL dataset, such as wind turbine power curve selection and PV panel specifications, have a greater impact on RES drought duration estimates than the precise geographic distribution of RES farms when studying the return periods of RES droughts.

The return periods calculated from the three datasets show large differences, in particular for the more extreme events with longer return periods. The C3S datasets produce shorter RES drought durations for these events, which would have the largest impact on the power system. This shows that system planning based on the wrong datasets could yield an underestimation of the duration of extreme RES droughts, potentially leading to shortages linked to undersized reserve capacity.

4.2.3. Seasonal Distribution of RES Droughts

The seasonal analysis of RES droughts is based on the percentage of hours in each month classified as part of a RES drought event. Wind droughts tend to be more frequent during summer, whereas solar PV droughts are more common in winter due to reduced sunlight. By comparing these seasonal patterns across different datasets and energy scenarios, this study examines how differences in model assumptions and capacity mix influence the characterisation of RES drought events. In Northwestern Europe, winter droughts are primarily driven by variations in wind generation, whereas summer droughts are mainly related to solar generation. This seasonal analysis is critical to ensure a cost-effective balance between generation and demand throughout the year.

For the wind-only scenario (Fig. 10a), the ATL dataset exhibits a pronounced seasonal pattern, with about 24% of summer hours (June, July, August) identified as RES droughts compared to only 4% in winter (December, January, February). This strong seasonal signal is less evident in the C3S datasets, which suggests that the differences in the underlying wind power curves play a significant role. In ATL, CF near or below the 0.1 threshold

occurs at relatively higher wind speeds, resulting in a higher count of RES drought hours during the summer months. In contrast, solar PV droughts (Fig. 10b) display an opposite seasonal trend. Across all datasets, over 60% of winter hours are classified as solar PV droughts, reflecting the naturally low solar irradiance in Ireland during winter.

ATL tends to record a slightly higher percentage of RES drought hours for wind and a marginally lower percentage for solar PV relative to the C3S datasets. These differences highlight how dataset-specific assumptions, such as the treatment of wind turbine power curves and PV panel characteristics, influences the seasonal dynamics of RES droughts.

The 91W-9PV scenario (Fig. 10c) shows patterns similar to the ones for wind droughts (Fig. 10a). However, in the 91W/9PV scenario, the number of hours classified as RES droughts in summer decreases slightly compared to the wind-only scenario. This reduction can be explained by the contribution of solar PV generation during the summer months in the 91W-9PV scenario, even though it constitutes only 9% of total capacity. Since the number of RES drought hours for solar PV in summer is near zero, this small contribution has a noticeable impact on reducing overall RES drought hours. In the 57W-43PV scenario (Fig. 10d), all three datasets show a reduction in monthly RES drought frequency. Annual reductions in median RES drought frequency are observed across the datasets, dropping from 14% to 5% for ATL, from 8% to 3% for C3S GRD, and from 9% to 4% for C3S NAT. The balanced mix of wind and solar PV power in this scenario reduces the seasonal signal overall and significantly decreases the percentage of RES drought hours in the summer.

The seasonal variations of RES droughts observed in this study have important implications for energy planning. Energy demand peaks in winter for Northern European countries, making the seasonality of RES droughts critical for the sizing of reserve capacity. Our results show that selecting the wrong dataset could severely underestimate RES droughts during winter months, thereby affecting the reliability of the energy system during critical periods. Additionally, the integration of large shares of solar PV in the system leads to a generalised reduction of RES droughts, yet winter months present a slight increase. The natural limitations of solar PV lead to inevitably higher reserve capacity needs during winter months as reliance on RES increases. These types of insights are essential to develop targeted strategies that enhance grid resilience and ensure a stable energy supply throughout the year.

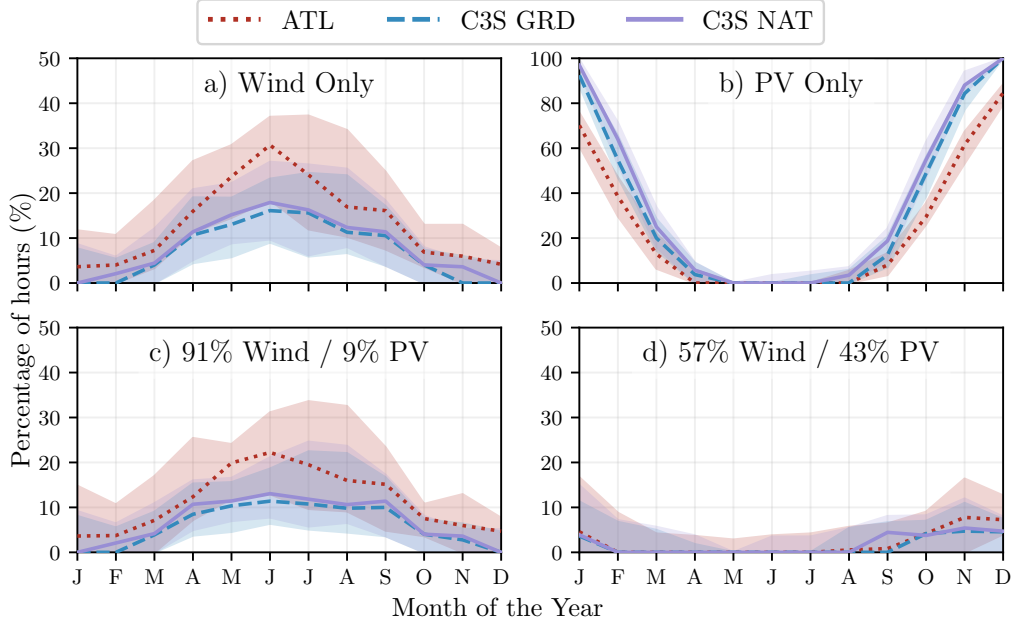


Figure 10: Percentage of hours in a month which are part of a RES drought (from 1979 to 2023) for a) Wind, b) Solar PV, c) 91W-9PV and d) 57W-43PV for ATL (red dotted), C3S GRD (blue dashed), and C3S NAT (purple solid). The x-axis represents the month of the year, and the y-axis indicates the percentage of hours. Lines correspond to the median values and the area between the first and third quartiles is shaded. Note the different y-axis scale for b).

5. Conclusions

This study aimed to answer two key questions: Do generic datasets have sufficient skill to reliably quantify RES drought events? How does the integration of solar PV into a predominantly wind-based system alter the characteristics of RES droughts? To address these questions, three datasets were compared: two derived from the European C3S-Energy dataset, and one developed by the authors. The datasets derived from C3S-Energy differ in their assumptions, one assumes a homogeneous distribution of wind and solar PV capacity across the region, while the other includes the actual locations of RES farms. The dataset developed by the authors uses a regionally validated model which accounts for farm locations and uses tailored wind and solar PV models selected to represent the actual generation.

Our results demonstrate that datasets without regional validation mis-

523 represent the frequency and duration of RES drought events due to their
524 limited ability to reproduce the observations. The inclusion of wind and so-
525 lar PV farm locations has limited impact on RES drought analysis compared
526 to the choice of wind turbine power curves and solar PV models. Whereas
527 all three datasets capture broad trends in the duration and seasonality of
528 RES drought events, the actual number of events is consistently underesti-
529 mated by the non-validated datasets. This effect becomes clearer for extreme
530 events, as not using regionally validated datasets can yield an overestimation
531 of the return periods of RES droughts. This can lead to insufficient reserve
532 capacity planning and potential risks to grid stability and security of supply.

533 The effect of adding solar PV capacity to a wind dominated power system,
534 as is currently happening in Northwestern Europe, has been explored in the
535 context of RES droughts. Our analysis has demonstrated that transitioning
536 to a system with more equal amounts of wind and solar PV capacity reduces
537 the occurrence of RES drought events, mitigates extreme RES drought condi-
538 tions and enhances overall system resilience. This improvement is attributed
539 to the complementary nature of wind and solar PV generation, as solar PV
540 generation typically peaks in summer while wind generation predominates
541 during winter. However, this integration is unable to counter critical win-
542 ter RES droughts, which coincide with the strongest electricity demand in
543 Northern European countries.

544 The results presented in this study have three main limitations. First,
545 the definition of RES droughts based on generation does not consider the
546 important role of demand, which could be of interest to system operators.
547 Second, recent solar PV capacity expansions have changed the generation
548 profile, limiting solar PV data for model training to a single year, although a
549 longer validation period would be preferable. Third, the source for weather
550 data is ERA5 which has limited spatial resolution, an issue that can be
551 addressed once higher resolution datasets become available.

552 Future work is planned to extend the current analysis. First, climate pro-
553 jection data will be integrated with different energy scenarios, incorporating
554 the addition of offshore wind, to better understand how climate change and
555 offshore wind may affect RES droughts. Second, expanding the geographic
556 domain of the study to include the rest of Europe, while also including the
557 role of electricity interconnects between countries, would provide a more com-
558 prehensive understanding of RES droughts. This would require extensive
559 verification across other European countries, making it a more complex but
560 highly relevant challenge.

561 Data Availability

562 The ERA5 data can be obtained from the Climate Data Store (<https://doi.org/10.24381/cds.adbb2d47>). The C3SE dataset is also available
563 from the Climate Data Store (<https://doi.org/10.24381/cds.4bd77450>).
564 Information on wind and solar PV farms in Ireland can be obtained from
565 the EirGrid website (<https://www.eirgrid.ie/grid/system-and-renewable-data-reports>). The Atlite model used in this study is open-source
566 and can be found on GitHub (<https://github.com/pypsa/atlite>). The
567 data and code required to reproduce the analysis in this article will be made
568 available upon acceptance of the manuscript in a public GitHub repository.
570

571 Acknowledgments

572 The research conducted in this publication was funded by Science Foun-
573 dation Ireland and co-funding partners under grant number 21/SPP/3756
574 through the NexSys Strategic Partnership Programme.

575 References

- 576 [1] EuroStat, Renewable Energy Statistics, 2023. URL: [https://ec.europa.eu/eurostat/statistics-explained/index.php?title=Renewable](https://ec.europa.eu/eurostat/statistics-explained/index.php?title=Renewable_energy_statistics)
577 [energy_statistics](https://ec.europa.eu/eurostat/statistics-explained/index.php?title=Renewable_energy_statistics), Accessed: 2024-11-06.
578
- 579 [2] I. Staffell, S. Pfenninger, The increasing impact of weather on electricity
580 supply and demand, *Energy* 145 (2018) 65–78.
- 581 [3] F. Kaspar, M. Borsche, U. Pfeifroth, J. Trentmann, J. Drücke, P. Becker,
582 A climatological assessment of balancing effects and shortfall risks of
583 photovoltaics and wind energy in germany and europe, *Advances in*
584 *Science and Research* 16 (2019) 119–128. doi:10.5194/asr-16-119-2
585 019.
- 586 [4] F. Mockert, C. M. Grams, T. Brown, F. Neumann, Meteorological
587 conditions during periods of low wind speed and insolation in Germany:
588 The role of weather regimes, *Meteorological Applications* 30 (2023)
589 e2141. doi:10.1002/met.2141.
- 590 [5] M. Ohba, Y. Kanno, D. Nohara, Climatology of dark doldrums in japan,
591 *Renewable and Sustainable Energy Reviews* 155 (2022) 111927. doi:10
592 .1016/j.rser.2021.111927.

- 593 [6] M. J. Mayer, B. Biró, B. Szücs, A. Aszódi, Probabilistic modeling of
594 future electricity systems with high renewable energy penetration using
595 machine learning, *Applied Energy* 336 (2023) 120801. doi:10.1016/j.
596 *apenergy*.2023.120801.
- 597 [7] D. Raynaud, B. Hingray, B. François, J. Creutin, Energy droughts from
598 variable renewable energy sources in European climates, *Renewable*
599 *Energy* 125 (2018) 578–589. doi:[https://doi.org/10.1016/j.renene](https://doi.org/10.1016/j.renene.2018.02.130)
600 *.2018.02.130*.
- 601 [8] A. Gangopadhyay, A. K. Seshadri, N. J. Sparks, R. Toumi, The role
602 of wind-solar hybrid plants in mitigating renewable energy-droughts,
603 *Renewable Energy* 194 (2022) 926–937. doi:10.1016/j.*renene*.2022.
604 *05.122*.
- 605 [9] J. Kapica, J. Jurasz, F. A. Canales, H. Bloomfield, M. Guezgouz,
606 M. De Felice, Z. Kobus, The potential impact of climate change on
607 european renewable energy droughts, *Renewable and Sustainable En-*
608 *ergy Reviews* 189 (2024) 114011. doi:10.1016/j.*rser*.2023.114011.
- 609 [10] K. Z. Rinaldi, J. A. Dowling, T. H. Ruggles, K. Caldeira, N. S. Lewis,
610 Wind and Solar Resource Droughts in California Highlight the Benefits
611 of Long-Term Storage and Integration with the Western Interconnect,
612 *Environmental Science and Technology* 55 (2021) 6214–6226. doi:10.1
613 *021/acs.est.0c07848*.
- 614 [11] P. T. Brown, D. J. Farnham, K. Caldeira, Meteorology and climatology
615 of historical weekly wind and solar power resource droughts over western
616 North America in ERA5, *SN Applied Sciences* 3 (2021) 814. doi:10.1
617 *007/s42452-021-04794-z*.
- 618 [12] S. Allen, N. Otero, Standardised indices to monitor energy droughts,
619 *Renewable Energy* 217 (2023) 119206. doi:10.1016/j.*renene*.2023.11
620 *9206*.
- 621 [13] C. Bracken, N. Voisin, C. D. Burleyson, A. M. Campbell, Z. J. Hou,
622 D. Broman, Standardized benchmark of historical compound wind and
623 solar energy droughts across the Continental United States, *Renewable*
624 *Energy* 220 (2024) 119550. doi:[https://doi.org/10.1016/j.renene](https://doi.org/10.1016/j.renene.2023.119550)
625 *.2023.119550*.

- [14] H. Lei, P. Liu, Q. Cheng, H. Xu, W. Liu, Y. Zheng, X. Chen, Y. Zhou, Frequency, duration, severity of energy drought and its propagation in hydro-wind-photovoltaic complementary systems, *Renewable Energy* (2024) 120845. doi:10.1016/j.renene.2024.120845, 2.
- [15] H. Hersbach, B. Bell, P. Berrisford, S. Hirahara, A. Horányi, J. Muñoz-Sabater, J. Nicolas, C. Peubey, R. Radu, D. Schepers, et al., The ERA5 global reanalysis, *Quarterly Journal of the Royal Meteorological Society* 146 (2020) 1999–2049. doi:10.1002/qj.3803.
- [16] L. Dubus, Y. Saint-Drenan, A. Troccoli, M. De Felice, Y. Moreau, L. Ho-Tran, C. Goodess, R. Amaro E Silva, L. Sanger, C3S Energy: A climate service for the provision of power supply and demand indicators for Europe based on the ERA5 reanalysis and ENTSO-E data, *Meteorological Applications* 30 (2023) e2145. doi:10.1002/met.2145.
- [17] F. Hofmann, J. Hampp, F. Neumann, T. Brown, J. Hörsch, Atlite: a lightweight Python package for calculating renewable power potentials and time series, *Journal of Open Source Software* 6 (2021) 3294. doi:10.21105/joss.03294.
- [18] A. Kies, B. U. Schyska, M. Bilousova, O. El Sayed, J. Jurasz, H. Stoecker, Critical review of renewable generation datasets and their implications for european power system models, *Renewable and Sustainable Energy Reviews* 152 (2021) 111614. doi:10.1016/j.rser.2021.111614.
- [19] EirGrid & SONI, System and Renewable Data Reports, 2023. URL: <https://www.eirgrid.ie/grid/system-and-renewable-data-reports>, Accessed: 2024-11-06.
- [20] Y.-M. Saint-Drenan, L. Wald, T. Ranchin, L. Dubus, A. Troccoli, An approach for the estimation of the aggregated photovoltaic power generated in several European countries from meteorological data, *Advances in Science and Research* 15 (2018) 51–62. doi:10.5194/asr-15-51-2018.
- [21] I. Staffell, S. Pfenninger, Using bias-corrected reanalysis to simulate current and future wind power output, *Energy* 114 (2016) 1224–1239. doi:10.1016/j.energy.2016.08.068.

- 659 [22] Government of Ireland, Climate Action Plan 2024, Technical Report 3,
660 Department of the Environment, Climate and Communications, 2023.
661 URL: [https://www.gov.ie/pdf/?file=https://assets.gov.ie/](https://www.gov.ie/pdf/?file=https://assets.gov.ie/284675/70922dc5-1480-4c2e-830e-295afd0b5356.pdf)
662 [284675/70922dc5-1480-4c2e-830e-295afd0b5356.pdf](https://assets.gov.ie/284675/70922dc5-1480-4c2e-830e-295afd0b5356.pdf), Accessed:
663 2024-11-06.
- 664 [23] Sustainable Energy Authority Ireland, National Energy Projections
665 2024, Technical Report, Sustainability Energy Authority of Ireland,
666 2024. URL: [https://www.seai.ie/news-and-events/news/energ](https://www.seai.ie/news-and-events/news/energy-projections-report)
667 [y-projections-report](https://www.seai.ie/news-and-events/news/energy-projections-report), Accessed: 2024-11-06.
- 668 [24] EirGrid & SONI, Tomorrow's Energy Scenarios 2023, Technical Report,
669 EirGrid & SONI, 2023. URL: [https://cms.eirgrid.ie/sites/def](https://cms.eirgrid.ie/sites/default/files/publications/TES-2023-Final-Full-Report.pdf)
670 [ault/files/publications/TES-2023-Final-Full-Report.pdf](https://cms.eirgrid.ie/sites/default/files/publications/TES-2023-Final-Full-Report.pdf),
671 Accessed: 2024-11-06.
- 672 [25] H. G. Beyer, G. Heilscher, S. Bofinger, A robust model for the mpp
673 performance of different types of pv-modules applied for the performance
674 check of grid connected systems, Eurosun (2004) 8.